THE JOURNAL OF BIOLOGICAL CHEMISTRY VOL. 281, NO. 1, pp. 626–637, January 6, 2006

Increased Proliferation and Altered Growth Factor Dependence of Human Mammary Epithelial Cells Overexpressing the Gab2 Docking Protein*

Received for publication, August 31, 2005, and in revised form, October 18, 2005 Published, JBC Papers in Press, October 27, 2005, DOI 10.1074/jbc.M509567200

Tilman Brummer[1], Daniel Schramek[1,2], Vanessa M. Hayes[3], Haley L. Bennett[4], C. Elizabeth Caldon[5], Elizabeth A. Musgrove[3], and Roger J. Daly[6]

From the Cancer Research Program, Garvan Institute of Medical Research, Sydney, New South Wales 2010, Australia

The docking protein Gab2 is a proto-oncogene product that is overexpressed in primary breast cancers. To determine the functional consequences of Gab2 overexpression, we utilized the immortalized human mammary epithelial cell line MCF-10A. In monolayer culture, expression of Gab2 at levels comparable with those detected in human breast cancer cells accelerated epidermal growth factor (EGF)-induced cell cycle progression and was associated with increased basal Stat5 tyrosine phosphorylation and enhanced and/or more sustained EGF-induced Erk and Akt activation. Three-dimensional Matrigel culture of MCF-10A cells resulted in the formation of polarized, growth-arrested acini with hollow lumina. Under these conditions, Gab2 increased cell proliferation during morphogenesis, leading to significantly larger acini, an effect dependent on Gab2 binding to Grb2 and Shp2 and enhanced by recruitment of the p85 subunit of phosphatidylinositol 3-kinase. Pharmacological inhibition of MEK revealed that, in addition to direct activation of phosphatidylinositol 3-kinase, increased Erk signaling also contributed to Gab2-mediated enhancement of acinar size. In addition, Gab2 overcame the proliferative suppression that normally occurs in late stage cultures and conferred independence of the morphogenetic program from exogenous EGF. Finally, higher levels of Gab2 expression led to the formation of large disorganized structures with defective luminal clearance. These findings support a role for Gab2 in mammary tumorigenesis.

Docking proteins represent an important class of signal transducer utilized by receptor and receptor-associated tyrosine kinases (1). Upon receptor activation, these proteins localize to the plasma membrane via an N-terminal domain (*e.g.* a pleckstrin homology domain in the case of Gab[7]/DOS proteins) and, following tyrosine phosphorylation at multiple sites, act to recruit a variety of SH2 domain-containing signaling proteins. Docking proteins thereby function as plasma membrane-proximal assembly platforms that mediate signal localization, amplification, and integration. The Gab/DOS family of docking proteins is represented by three paralogs in mammals (Gab1–3) and one ortholog each in *Drosophila* (DOS) and *Caenorhabditis* (SOC-1) (2, 3). Tyrosine phosphorylation of Gab proteins has been reported in response to activation of a plethora of cell-surface receptors, including several classes of receptor tyrosine kinases, T- and B-cell antigen receptors, RANK, and β_1-integrins (2–5). Although Gab1 can bind the c-Met receptor tyrosine kinase directly (6), association of Gab1 and Gab2 with receptor signaling complexes is often mediated by the adaptor protein Grb2 (3). The latter binds the tyrosine-phosphorylated receptor or a receptor-associated protein via its SH2 region and the Gab protein via its C-terminal SH3 domain. An important signaling function of Gab proteins is to bind and activate the protein-tyrosine phosphatase Shp2, resulting in enhanced and/or more sustained Ras/Erk signaling (3). Shp2 can positively regulate Ras activation by dephosphorylating Ras GTPase-activating protein recruitment sites on the EGFR (7) or Gab1 (8) or by indirectly activating Src family tyrosine kinases via dephosphorylation of Csk-binding sites on paxillin (9) or PAG/Cbp (10). A second key pathway downstream of Gab proteins is activation of PI3K because Gab1–3 exhibit three Y*XX*M motifs that mediate recruitment of the p85 subunit of this enzyme. In addition, Gab1 and Gab2 both bind Crk adaptors, and Gab1 couples to phospholipase Cγ (2, 3).

Although Gab3-deficient mice lack an obvious phenotype, suggesting functional redundancy with the other family members (11), Gab1 and Gab2 perform unique functions in normal and pathological states. *Gab1* gene knockouts display embryonic lethality, probably due to the key role played by Gab1 in Met signaling (12, 13). In contrast, mice lacking Gab2, which has a more tissue-specific expression pattern, exhibit impaired mast cell-mediated allergic responses and osteoclast differentiation due to a requirement for Gab2 downstream of Fcϵ receptor I and RANK, respectively (5, 14). Furthermore, Gab2 is strongly implicated in oncogenic signaling. Gab2 S159A, which is uncoupled from negative feedback phosphorylation by Akt, displays potent transforming properties in fibroblasts, identifying Gab2 as a proto-oncogene product (15). Also, Gab2 is essential for the transformation of fibroblasts by the v-Sea tyrosine kinase oncoprotein (16) and of myeloid cells by Bcr-Abl (17) or Shp2 E76K, a mutated hyperactive version of Shp2 found in certain leukemias (18). Finally, Gab2 is overexpressed in breast cancer cell lines and primary breast cancer specimens (19).

It is now well established that signaling by specific receptor tyrosine kinases plays key roles in both mammary gland development and tumorigenesis. For example, in the normal mammary gland, the ErbB receptor signaling network functions in ductal outgrowth, alveolar morphogenesis, and lactation (20), whereas in breast cancer, overexpression

* This work was supported in part by Department of Defense Breast Cancer Research Program Grant DAMD17-00-1-0251 and by grants from the National Health and Medical Research Council of Australia, the Cancer Council NSW, and the Association for International Cancer Research. The costs of publication of this article were defrayed in part by the payment of page charges. This article must therefore be hereby marked "*advertisement*" in accordance with 18 U.S.C. Section 1734 solely to indicate this fact.

[1] Both authors contributed equally to this work.
[2] Recipient of an Endeavor Australian postgraduate research fellowship.
[3] Cancer Institute NSW Fellow.
[4] Recipient of an Australian postgraduate award.
[5] Cancer Institute NSW Scholar and recipient of an Australian postgraduate award.
[6] To whom correspondence should be addressed: Cancer Research Program, Garvan Inst. of Medical Research, 384 Victoria St., Sydney, New South Wales 2010, Australia. Tel.: 61-2-9295-8333; Fax: 61-2-9295-8321; E-mail: r.daly@garvan.org.au.

[7] The abbreviations used are: Gab, Grb2-associated binder; DOS, daughter of Sevenless; SH, Src homology; RANK, receptor activator of NF-κB; Grb2, growth factor receptor-bound 2; Erk, extracellular signal-regulated kinase; EGFR, epidermal growth factor receptor; PI3K, phosphatidylinositol 3-kinase; EGF, epidermal growth factor; HA, hemagglutinin; GFP, green fluorescent protein; Stat, signal transducer and activator of transcription; Rb, retinoblastoma protein; MEK, mitogen-activated protein kinase/extracellular signal-regulated kinase kinase.

of either EGFR/ErbB1 or ErbB2 is associated with a more aggressive disease phenotype (21). Consequently, given the oncogenic potential of Gab2 and its common overexpression in breast cancers, an important unresolved question is the functional consequences of elevated Gab2 expression in normal mammary epithelial cells. To address this, we have exploited the characteristics of the spontaneously immortalized human mammary epithelial cell line MCF-10A. Upon three-dimensional culture in reconstituted basement membrane (Matrigel), these cells form acinar structures that retain important characteristics of glandular epithelium *in vivo*, such as apicobasal polarization, suppression of proliferation, and acinar cavitation through apoptosis of cells located within the inner cell mass (22). This three-dimensional culture system provides a powerful model for characterizing the biological activities of proteins implicated in breast cancer development and progression. Effects observed upon overexpression and/or constitutive activation of particular oncoproteins include lack of proliferative suppression (cyclin D_1), luminal filling, development of multiacinar structures (ErbB2), and disruption of cell-cell adhesion in acini (colony-stimulating factor receptor) (23–25). In this study, we demonstrate that, depending on its expression level in MCF-10A cells, Gab2 is capable of conferring increased acinar size, resistance to proliferative suppression within acinar structures, independence of the morphogenetic program from exogenous EGF, and defective luminal clearance, thus supporting a role for Gab2 in breast cancer development.

EXPERIMENTAL PROCEDURES

Mutation Detection—Genomic DNA was extracted from 32 cancer cell lines (17 breast, 12 ovarian, and three prostate) and four cell lines from normal breast tissue using conventional methods. Detection of genetic variation was performed using PCR-based denaturing gradient gel electrophoresis (26, 27) for the entire coding region (exons 2–10), including splice junctions, of the *GAB2* gene.[8] Amplified products showing aberrant denaturing gradient gel electrophoresis banding patterns were subjected to automated sequencing using an ABI 3100 gene analyzer (Applied Biosystems).

Retroviral Vectors—A cDNA insert encoding human Gab2 with a C-terminal HA tag was excised from pcDNA3.1/Gab2-HA [9] by XbaI/HindIII digestion, blunted, and subcloned into the HpaI site of the retroviral vector pMIG (also known as pMSCV-IRES-GFP (28)) to yield the construct pMIG/Gab2. The QuikChange site-directed mutagenesis kit (Stratagene) was used to generate pMIG/Gab2 expression vectors encoding Gab2 mutants lacking the binding sites for Grb2 (ΔGrb2), p85 (Δp85), and Shp2 (ΔShp2). In brief, the ΔGrb2 mutant was generated by deleting the ^{351}PPPRPPKP^{358} sequence, representing a typical Grb2-binding site, and by performing two alanine substitutions to mutate the atypical Grb2-binding site from ^{510}PPPVNR^{515} to PAPVNA (29). The other mutants were generated by performing phenylalanine substitutions at Tyr^{614} and Tyr^{643} (ΔShp2) and Tyr^{452}, Tyr^{476}, and Tyr^{584} (Δp85).[10] The coding sequences of all Gab2 mutants were confirmed by DNA sequencing.

Cell Culture and Retroviral Infection of MCF-10A Cells—Monolayer cultures of MCF-10A cells were maintained in Dulbecco's modified Eagle's medium/nutrient mixture F-12 (Invitrogen) supplemented with 5% (v/v) horse serum (Invitrogen), 20 ng/ml human recombinant EGF (R&D Systems), 0.5 μg/ml hydrocortisone (Sigma), 100 ng/ml cholera toxin (Sigma), 10 μg/ml bovine insulin (Sigma), 50 units/ml penicillin G (Invitrogen), and 50 μg/ml streptomycin sulfate (Invitrogen). For growth factor stimulation experiments, cells were starved overnight in 0.2% (v/v) horse serum prior to treatment with 10 ng/ml EGF. For cell cycle analysis of cells grown in monolayer culture, MCF-10A cells were starved for 34 h in 0.2% (v/v) horse serum and then stimulated with 10 ng/ml EGF. Relative cell numbers were estimated using a non-radioactive cell proliferation assay (Promega) after up to 5 days of EGF treatment, and doubling times were calculated from lines of best fit during exponential growth.

For the establishment of three-dimensional cultures, cells grown in monolayer culture were detached by trypsin/EDTA treatment and seeded in precoated glass chamber slides as described previously (30). Briefly, cells were washed once with phosphate-buffered saline and then resuspended in assay medium (Dulbecco's modified Eagle's medium/nutrient mixture F-12 supplemented with 2% (v/v) horse serum, cholera toxin, hydrocortisone, penicillin G, and streptomycin sulfate as described above) at 2.5×10^4 cells/ml. 8- or 4-well glass chamber slides were coated with 40 or 80 μl of Matrigel/well, respectively, and left to solidify in the incubator for 1 h. The cells were then mixed with an equal volume of assay medium containing 4% (v/v) Matrigel, which was supplemented with 10 ng/ml EGF and 10 μg/ml insulin or with either EGF or insulin alone. The cell suspension was then added to the 4- or 8-well chamber slides to yield 5×10^3 or 1×10^4 cells/well, respectively. This time point was taken as Day 0, and the medium was replaced every 4 days. For preparation of cell lysates from the three-dimensional culture, the appropriate medium was replaced at Day 3, and cells were recovered and lysed at Day 4 as described below. Where indicated, U0126 (Promega Corp.) was added to cultures at the specified dose on Day 1, and the medium was replaced on Day 3.

MCF-10A cells expressing the ecotropic retroviral receptor (MCF-10A/EcoR cells; a kind gift of Drs. Danielle Lynch and Joan Brugge) were grown and infected with retroviruses as described (30). In brief, the ecotropic packing cell line Phoenix-Eco was transfected with 10 μg of plasmid DNA using PolyFect (Qiagen Inc.). Retroviral supernatants were collected 48 h post-transfection, passed through a 0.22-μm filter, supplemented with Polybrene at a final concentration of 8 μg/ml, and diluted with fresh MCF-10A growth medium. This solution was then used to overlay a subconfluent culture of MCF-10A/EcoR cells, which were plated out at a density of 5×10^6 cells/10-cm dish on the day before infection. GFP-positive cells were then sorted to homogeneity by flow cytometry.

Antibodies—Antibodies against phospho-Thr^{308} Akt, phospho-Ser^{473} Akt, total Akt, and phosphorylated and total p42/44 Erk and Stat5 were purchased from Cell Signaling Technology. Rat anti-HA monoclonal antibody 3F10 was obtained from Roche Diagnostics. Horseradish peroxidase-conjugated anti-phosphotyrosine antibody PY20 and antibodies against β-catenin (clone 14) and E-cadherin (clone 36) were obtained from BD Transduction Laboratories. Antibodies against the EGFR (528 or 1005) and Rb (C-15) were purchased from Santa Cruz Biotechnology, Inc. The anti-Gab2 (B-D39), anti-phospho-Rb (S780), anti-activated caspase-3, anti-β-actin (clone AC-15), and anti-Ki67 antibodies were purchased from Diaclone, Calbiochem, R&D systems, Sigma, and DakoCytomation, respectively.

Analysis of Three-dimensional Matrigel Cultures by Bright-field and Confocal Microscopy—Acini were photographed, and their diameters were assessed using Leica Q500 MC QWin software (Version V01.02). For confocal microscopy, the acini were fixed and stained using the indicated antibodies as described (30). Following incubation with the primary antibodies, the acini were stained using the appropriate Cy3-labeled secondary antibodies (Jackson ImmunoResearch Laboratories,

[8] Primer sequences and denaturing gradient gel electrophoresis conditions are available on request.
[9] D. K. Lynch and R. J. Daly, unpublished data.
[10] Primer details are available upon request.

Inc.) and TOPRO-3 or 4′,6-diamidino-2-phenylindole as a DNA counterstain.

Recovery of Acini from Three-dimensional Matrigel Cultures—After removal of the supernatant, the cultures were incubated in an appropriate volume of cell recovery solution (BD Biosciences) for 75 min at 4 °C to dissolve the Matrigel. Thereafter, acini were collected by centrifugation at 805 × *g* for 10 min at 4 °C and washed once with cold phosphate-buffered saline.

Cell Lysis and Immunoprecipitation—Recovered acini or cells grown in monolayer culture were washed once with ice-cold phosphate-buffered saline and lysed with radioimmune precipitation assay buffer (50 mM HEPES (pH 7.4), 1% (v/v) Triton X-100, 0.5% (w/v) sodium deoxycholate, 0.1% (w/v) SDS, 50 mM sodium fluoride, 5 mM EDTA, 1 mM phenylmethylsulfonyl fluoride, 10 μg/ml aprotinin, 10 μg/ml leupeptin, and 1 mM sodium orthovanadate) for 10 min on ice. Thereafter, the suspension was centrifuged at 17,530 × *g* for 15 min at 4 °C, and the supernatant was transferred into a fresh tube and stored at −80 °C.

For the immunoprecipitation of Gab2 signaling complexes, a subconfluent 10-cm dish of MCF-10A cells expressing the indicated Gab2 proteins was lysed with 1 ml of lysis buffer (1% (v/v) Triton X-100, 50 mM HEPES (pH 7.5), 150 mM NaCl, 10% (v/v) glycerol, 1.5 mM $MgCl_2$, 1 mM EGTA, 10 mM sodium pyrophosphate, 20 mM NaF, 1 mM phenylmethylsulfonyl fluoride, 1 mM sodium orthovanadate, 10 μg/ml aprotinin, and 10 μg/ml leupeptin) for 15 min. Subsequently, immunoprecipitations were performed by adding 1 μg of anti-HA monoclonal antibody to 900 μl of post-nuclear supernatant containing 50 μl of recombinant protein G-Sepharose 4B slurry (Zymed Laboratories Inc.) as described previously (31). Following overnight incubation, the immunoprecipitates were washed four times with lysis buffer and then resuspended in SDS-PAGE sample buffer.

Western Blot Analysis—This was performed as described previously (32).

Flow Cytometry—Cells grown in monolayer culture or recovered acini were trypsinized at 37 °C for 12 min. Subsequently, the trypsin was inactivated by adding harvest medium (Dulbecco's modified Eagle's medium supplemented with 2% horse serum), and cells were collected by centrifugation at 805 × *g* for 5 min at 4 °C. Thereafter, cells were resuspended in harvest medium containing 62.5 μg/ml ethidium bromide and 0.25% (v/v) Triton X-100 and incubated at room temperature in the dark for 3 h. 2 h before fluorescence-activated cell sorting analysis, RNase (Sigma) was added to a final concentration of 500 μg/ml. All fluorescence-activated cell sorting data were acquired with a FACSCalibur (BD Biosciences) with CellQuest professional software. Analysis was performed with ModFit software.

Densitometry—This was performed using IPLab Gel software (Signal Analytics Inc.).

Statistical Analysis—This utilized a two-sided Student's *t* test, and differences were considered to be statistically significant at $p < 0.05$. For statistical evaluation of more than two groups, analysis of variance was used. A Ryan-Einot-Gabriel-Welsch multiple comparison test was employed to compare every possible pair of means and to distinguish significantly different groups using SPSS software.

RESULTS

Overexpression of Gab2 in the Immortalized Human Mammary Epithelial Cell Line MCF-10A—Prior to commencing our functional analysis of Gab2, it was important to determine whether the *GAB2* gene is mutated in breast cancer cell lines, leading to expression of Gab2 proteins with enhanced transforming potential (*e.g.* Gab2 S159A (15)). All of the nine coding exons and the corresponding intron-exon boundaries of the *GAB2* gene were screened for mutations in 17 breast cancer cell lines; however, no changes affecting the Gab2 protein sequence were detected. Similarly, the *GAB2* coding sequence in 12 ovarian and three prostate cancer cell lines was not altered (data not shown). Although this does not rule out the possibility of a low frequency of *GAB2* mutations in primary breast cancers, these data led us to focus on the functional consequences of overexpressing the wild-type Gab2 protein in human mammary epithelial cells.

In our original study, we determined that normal or immortalized human mammary epithelial cells express very low levels of endogenous Gab2, whereas a subset of breast cancer cell lines exhibits Gab2 expression that is at least an order of magnitude higher (19). However, MCF-10A cells were not included in this analysis. Therefore, Western blotting was used to confirm that Gab2 expression in these cells was also low (Fig. 1*A* and data not shown). The cells were then infected with a bicistronic retrovirus encoding Gab2 and GFP from the same transcript and sorted according to their green fluorescence. This allowed the isolation of three pools expressing relatively low, medium, and high levels of Gab2 (Fig. 1*A*). These pools expressed levels of Gab2 that were 3-, 6-, and 18-fold higher, respectively, than those in the breast cancer cell line with the highest Gab2 expression, MDA-MB-468 (19). Therefore, the low expressing pool represented an appropriate model to study the biological consequences of Gab2 overexpression and was used for all of our analyses, unless indicated otherwise.

Effects of Gab2 Overexpression on EGF-induced Signaling and Cell Cycle Progression in Monolayer Culture—EGF is an important mitogen for MCF-10A cells in culture (33). Therefore, we first examined the effects of Gab2 overexpression on EGF-induced signaling events. Western blotting of cell lysates revealed reduced tyrosine phosphorylation of protein bands at ~180 and 110 kDa and increased phosphorylation of a band at 95 kDa in MCF-10A/Gab2 cells compared with controls (Fig. 1*B*). Immunoprecipitation/Western blot analysis identified the 180-kDa band as the EGFR (data not shown) and the 95-kDa band as Gab2 (see Fig. 4*A*), whereas the 110-kDa band remained uncharacterized. Because the total levels of the EGFR were unchanged (data not shown), reduced tyrosine phosphorylation of this receptor upon Gab2 overexpression is likely to reflect competition between phosphorylation sites on Gab2 and the EGFR C terminus. Furthermore, the activity of several downstream signaling pathways was enhanced in MCF-10A/Gab2 cells relative to controls. Phosphorylation of the PI3K effector Akt at the regulatory sites Thr^{308} and Ser^{473} was increased at both early and late time points (Fig. 1, *B* and *C*), whereas MCF-10A/Gab2 cells also exhibited more sustained Erk activation as indicated by increased levels of phospho-Erk at 15 and 45 min post-stimulation (Fig. 1, *B* and *D*). Finally, MCF-10A/Gab2 cells displayed a higher basal level of Stat5 tyrosine phosphorylation. (In three independent experiments, there was a mean increase of 2.3-fold ($p < 0.05$).) This increased phosphorylation was maintained over 45 min of EGF stimulation.

To further characterize the functional consequences of Gab2 overexpression, we investigated growth factor regulation of the cell cycle. EGF treatment of cells arrested in G_1 phase by serum starvation led to a semisynchronous entry into S phase that was both more pronounced and more rapid for Gab2-overexpressing cells, so the percentage of cells in S phase peaked ~3 h earlier than for vector controls (Fig. 2). EGF stimulation led to sustained proliferation of both control and Gab2-overexpressing cells, with respective doubling times of 35.5 and 27.0 h at 0.1 ng/ml EGF and 15.5 and 14.2 h at 10 ng/ml EGF. Therefore, the increased activation of mitogenic signaling pathways in MCF-10A/Gab2 cells results in an enhanced rate of EGF-induced G_1 phase progression and a consequent increase in the overall rate of proliferation.

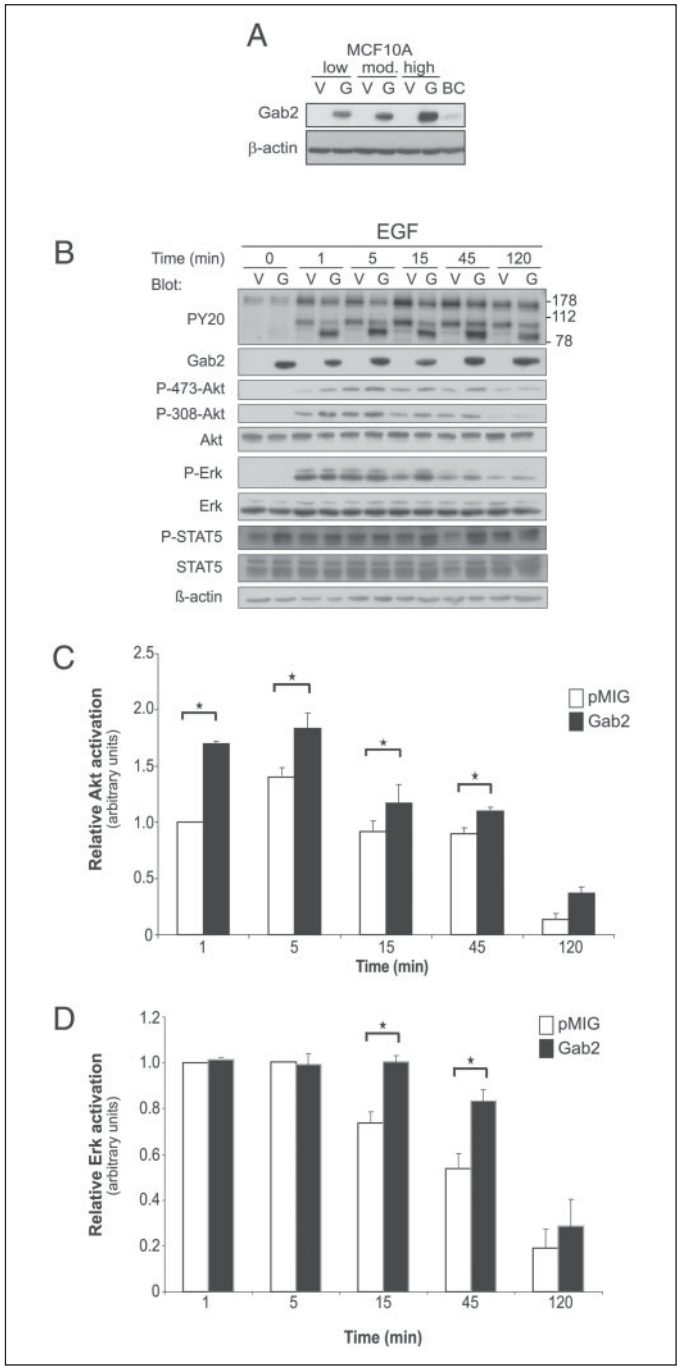

FIGURE 1. **Modulation of EGF-induced signaling in MCF-10A monolayers by Gab2.** *A*, Gab2 expression levels in retrovirally infected MCF-10A cells compared with human breast cancer cells. MCF-10A cells infected with the pMIG/Gab2 retrovirus (*G*) or the corresponding empty vector control (*V*) were sorted into three different fractions according to the GFP signal. The results from Western blot analysis of Gab2 expression in these pools and the Gab2-overexpressing breast cancer cell line MDA-MB-468 (*BC*) are shown. The lysates were also blotted for β-actin as a loading control. The low expressing pool was used for all experiments, unless indicated otherwise. *mod*, moderate. *B*, activation of specific signaling pathways. Gab2-overexpressing or control MCF-10A cells were serum-starved overnight and then stimulated with EGF for the indicated times. Cell lysates were subjected to Western blotting with the indicated antibodies. The mobilities of molecular mass standards (in kilodaltons) are indicated on the right. *P-473-Akt*, phospho-Ser^{473} Akt; *P-308-Akt*, phospho-Thr^{308} Akt; *P*, phospho. *C*, enhancement of EGF-induced Akt activation by Gab2 overexpression. Phosphorylation of Akt at Ser^{473} at each time point was quantified by densitometry, normalized for loading, and expressed relative to the signal for vector control cells at 1 min. *D*, effect of Gab2 overexpression on EGF-induced Erk activation. Phospho-Erk signals were quantified and analyzed as described for *C*. In *C* and *D*, the data were derived from four independent experiments The *error bars* represent S.E. *, $p < 0.05$, significant difference between vector- and Gab2-infected cells.

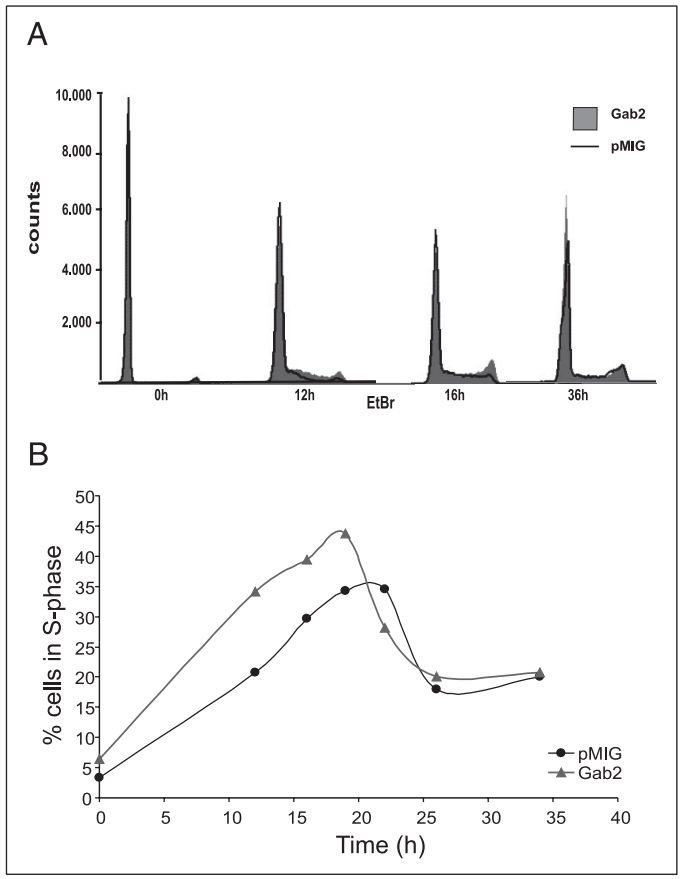

FIGURE 2. **Effect of Gab2 on EGF-induced cell cycle progression.** Subconfluent cultures of control (pMIG) and Gab2-overexpressing MCF-10A cells were serum-starved and then stimulated with EGF. DNA content was assayed by flow cytometry at different time points. The histograms (*A*) indicate the cell cycle phase distribution of the different cell populations at specific time points, whereas the graph (*B*) shows the corresponding percentage of cells in S phase *versus* time.

Effects of Gab2 Overexpression on Growth of MCF-10A Acini—Optimal acinar development by MCF-10A cells in three-dimensional Matrigel cultures requires the presence of both exogenous EGF and insulin (34). When grown in medium supplemented with both growth factors, MCF-10A/Gab2 cells formed acini that were significantly larger than those formed by vector control cells. This size difference was evident at Day 6 of culture and reached a maximum between Days 12 and 21, when the increase in acinar diameter was ~25% (Fig. 3, *A* and *B*). We also investigated acinar growth and morphogenesis in medium containing EGF alone. At Day 6 of culture, there was an increase in acinar diameter relative to controls of ~50%, indicating that, during the early stages of acinar development, Gab2 can partially substitute for the growth-promoting effect of insulin. Although the size of Gab2-overexpressing acini was near-maximal at Day 6, whereas the control acini continued to increase in size until Day 12, a significant increase in diameter for the former was still evident at Day 21. For cells grown in full growth medium or only in the presence of EGF, Gab2 overexpression did not impair luminal clearance in late stage cultures (Fig. 3*C*). However, staining at late time points for the proliferative marker Ki67 revealed a greater proportion of positive cells in Gab2-overexpressing acini (Fig. 3*D*), indicating that Gab2 overrides the proliferative suppression that normally occurs in the morphogenic program.

Western blot analysis of lysates derived from Day 4 acini grown in full growth medium or only in the presence of EGF revealed that Gab2 overexpression resulted in increased levels of phospho-Ser^{780} Rb (both

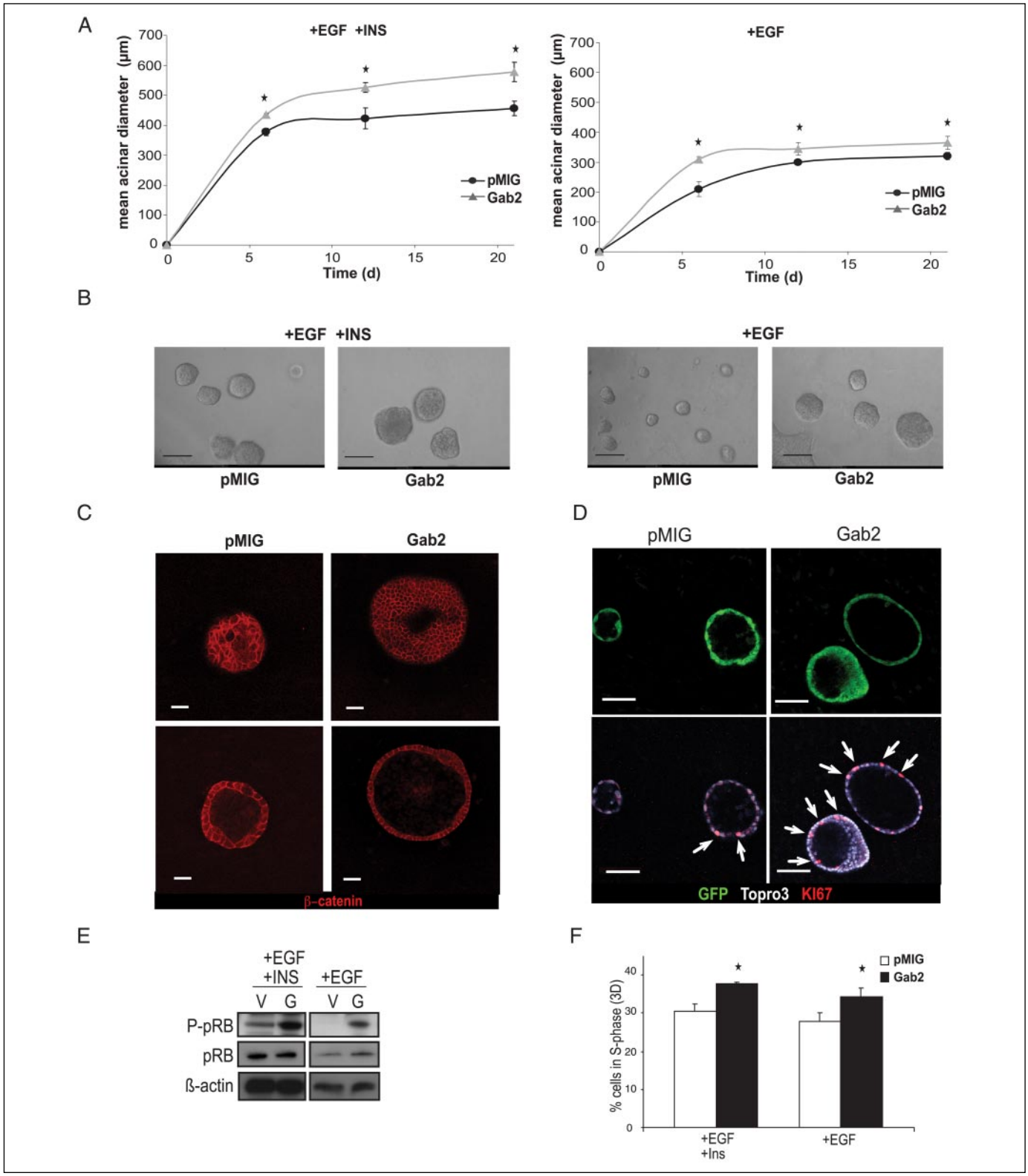

FIGURE 3. **Effect of Gab2 on the morphogenetic program in three-dimensional Matrigel culture.** *A* and *B*, effect of Gab2 on acinar diameter. Control or Gab2-overexpressing MCF-10A cells were maintained in three-dimensional Matrigel cultures either in full culture medium supplemented with EGF and insulin (*+EGF +INS*) or in medium supplemented with EGF only (*+EGF*), and the mean acinar diameter was assessed over 21 days. In *A*, each point represents the mean acinar diameter derived from three independent experiments. In each experiment, 150 structures were analyzed per time point. Representative phase-contrast images from cultures at Day 21 are shown in *B*. *Scale bars* = 500 μm. *C* and *D*, acinar morphogenesis. The *upper* and *lower panels* in *C* represent polar and equatorial confocal cross-sections, respectively, of acini stained for β-catenin. *Scale bars* = 40 μm. GFP fluorescence (*upper panels*) and staining for Ki67 and TOPRO-3 (*lower panels*) are shown for control and Gab2-overexpressing cultures in *D*. *Arrows* highlight Ki67-positive cells. *Scale bars* = 40 μm. *E* and *F*, effect of Gab2 on cell cycle progression in three-dimensional culture. In *E*, lysates from three-dimensional cultures at Day 4 were subjected to Western blotting with an antibody specific for Ser^{780}-phosphorylated Rb (*P-pRB*) and total Rb (*pRB*). β-Actin served as a loading control. *G*, Gab2; *V*, vector. In *F*, the cell cycle phase distribution of cells at Day 4 was determined by flow cytometry. The mean percentage of cells in S phase from three independent experiments is shown. For *A* and *F*, the *error bars* indicate S.E. *, $p < 0.05$, significant difference between vector- and Gab2-infected cells.

growth conditions) and total Rb (EGF alone) (mean 24% increase, $p = 0.03$), indicating enhanced signaling to the cell cycle machinery (Fig. 3*E*). Consistent with these data, flow cytometric analysis of the cell cycle phase distribution revealed that Gab2 overexpression resulted in a significant increase in the percentage of cells in S phase (Fig. 3*F*). This approach also revealed that Gab2 overexpression did not alter cell size (data not shown). Therefore, the observed increases in acinar size reflect enhanced proliferation within the Gab2-overexpressing structures, particularly during the early stages of acinar development.

Determination of the Signaling Requirements for Gab2-mediated Enhancement of Acinar Size—To characterize the function of Grb2 binding by Gab2 in the MCF-10A system, we generated a Gab2 mutant with both Grb2-binding sites deleted (ΔGrb2). Also, to determine the roles of two key Gab2 effectors, we generated Tyr-to-Phe mutants at the two Shp2-binding sites (ΔShp2) or three p85 recruitment sites (Δp85). The different mutants were expressed in MCF-10A cells by retroviral infection, and the GFP-positive fractions were subjected to flow cytometric sorting to isolate pools with expression comparable to that in MCF-10A/Gab2 cells.

First, we characterized the magnitude and kinetics of EGF-induced tyrosine phosphorylation of the different Gab2 proteins, with a particular focus on ΔGrb2. Western blotting of Gab2 immunoprecipitates confirmed loss of Grb2 binding for this mutant (Fig. 4*C*). Interestingly, at 2.5 min of EGF stimulation, all of the mutants exhibited a similar degree of tyrosine phosphorylation that was slightly reduced compared with the wild-type protein (Fig. 4*A*, *upper panels*). However, at 15 min, phosphorylation of ΔGrb2 was markedly reduced compared with phosphorylation of both Δp85 and ΔShp2, indicating more transient phosphorylation in the absence of Grb2 association (Fig. 4*A*, *lower panels*). Furthermore, association of the ΔGrb2 mutant with the receptor was reduced compared with wild-type Gab2 and the other mutants at 2.5, 15 and 30 min (Fig. 4*B* and data not shown), confirming that Grb2 acts to bridge the EGFR and Gab2 and suggesting that receptor association is required for sustained tyrosine phosphorylation of Gab2. Introduction of the ΔGrb2 mutations also abrogated ligand-induced Shc binding to Gab2 (Fig. 4*C*), indicating that Gab2-bound Grb2 normally acts to bind tyrosine-phosphorylated Shc via the Grb2 SH2 domain.

In terms of recruitment of other proteins, Shp2 binding to Gab2 peaked at 2.5 min and then gradually declined (Fig. 4*C* and data not shown). However, Shp2 recruitment was markedly reduced for the ΔGrb2 mutant and almost undetectable for the ΔShp2 mutant. Interestingly, ΔShp2 also exhibited reduced ligand-induced binding of Grb2. Binding of p85 was undetectable at 2.5 min, reached a maximum at 15 min, and then declined from 15 to 30 min (Fig. 4*D* and data not shown). Recruitment was reduced for ΔGrb2 and undetectable for Δp85. Thus, in line with its transient tyrosine phosphorylation, ΔGrb2 is impaired in its binding of two key Gab2 effectors.

The effect of the different mutants on acinar growth was then determined. For cells grown in three-dimensional culture in the presence of both EGF and insulin, acini derived from cells expressing the Δp85 mutant were consistently of an intermediate acinar diameter compared with those derived from control or Gab2-expressing cells (Figs. 5*A* and 6*D*). However, no effect on acinar size was observed for the ΔGrb2 and ΔShp2 mutants. Similar trends were observed in the presence of only EGF; but under these conditions, the effect of the Δp85 mutant was less marked (Fig. 5*A*).

To characterize the effects of Gab2 and the different mutants on cell signaling in three-dimensional culture, acini were recovered from the Matrigel, lysed, and subjected to Western blot analysis (Fig. 5*B*). Robust tyrosine phosphorylation of Gab2 was observed for cells grown with

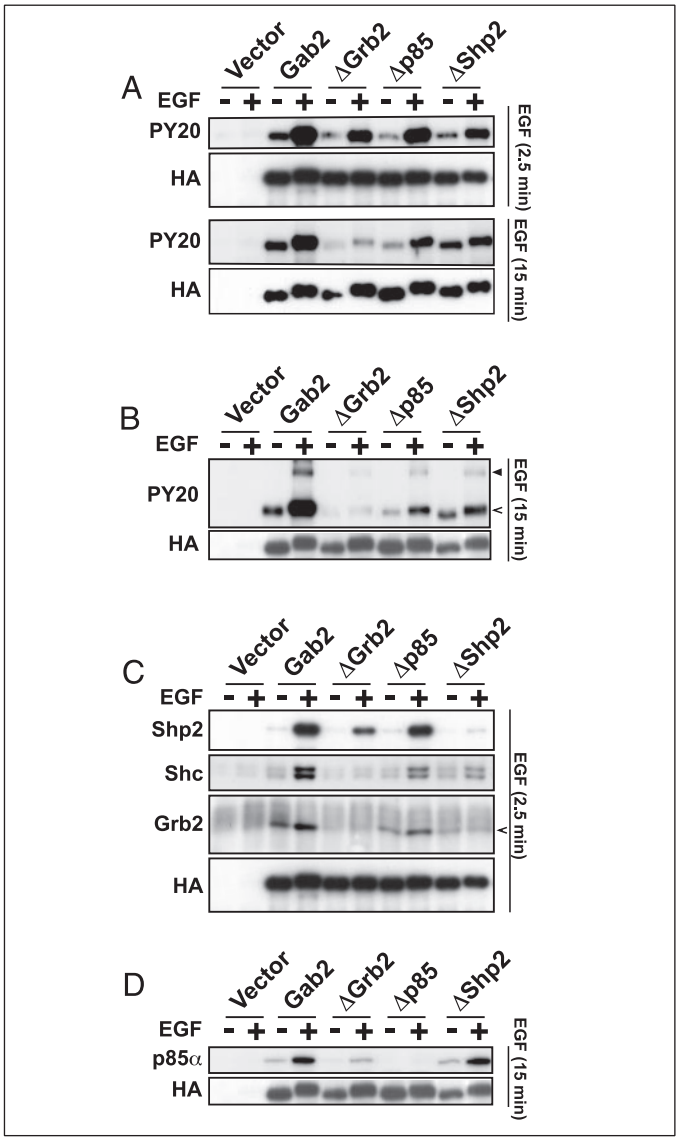

FIGURE 4. **Characterization of Gab2 binding site mutants.** *A*, Gab2 tyrosine phosphorylation. MCF-10A cells expressing HA-tagged wild-type Gab2 or the indicated mutants together with the corresponding vector control pool were stimulated with EGF for the indicated times. Anti-HA immunoprecipitates were then Western-blotted for phosphotyrosine (PY20) or HA as a loading control. *B*, association with the EGFR. A long exposure of an immunoprecipitation/Western blot experiment performed as described for *A* is shown. The *closed arrowhead* highlights co-immunoprecipitated EGFR, whereas the *open arrowhead* indicates Gab2. *C* and *D*, association with other proteins. Immunoprecipitates (as described for *A*) were Western-blotted with the indicated antibodies. The *open arrowhead* in *C* indicates the mobility of Grb2.

EGF and insulin or with EGF alone. Under both conditions, tyrosine phosphorylation of the Δp85 and ΔShp2 mutants was reduced, whereas that of the ΔGrb2 mutant was undetectable. This pattern was similar to that observed for cells maintained in monolayer culture and stimulated with EGF for 15 min (Fig. 4*A*). The levels of phospho-Erk in the vector controls were markedly reduced for cells grown with EGF compared with those maintained in the presence of EGF and insulin. However, under either culture condition, expression of either wild-type Gab2 or the Δp85 mutant resulted in an enhancement of Erk activation, which was not observed for either the ΔGrb2 or ΔShp2 mutant. For cells grown in EGF and insulin, the increases for wild-type Gab2 and the Δp85 mutant were 77 and 50% ($p < 0.01$), respectively, whereas for cells grown with EGF only, the increases were 117 and 126% ($p < 0.01$), respectively. Cells maintained in the presence of EGF and insulin exhib-

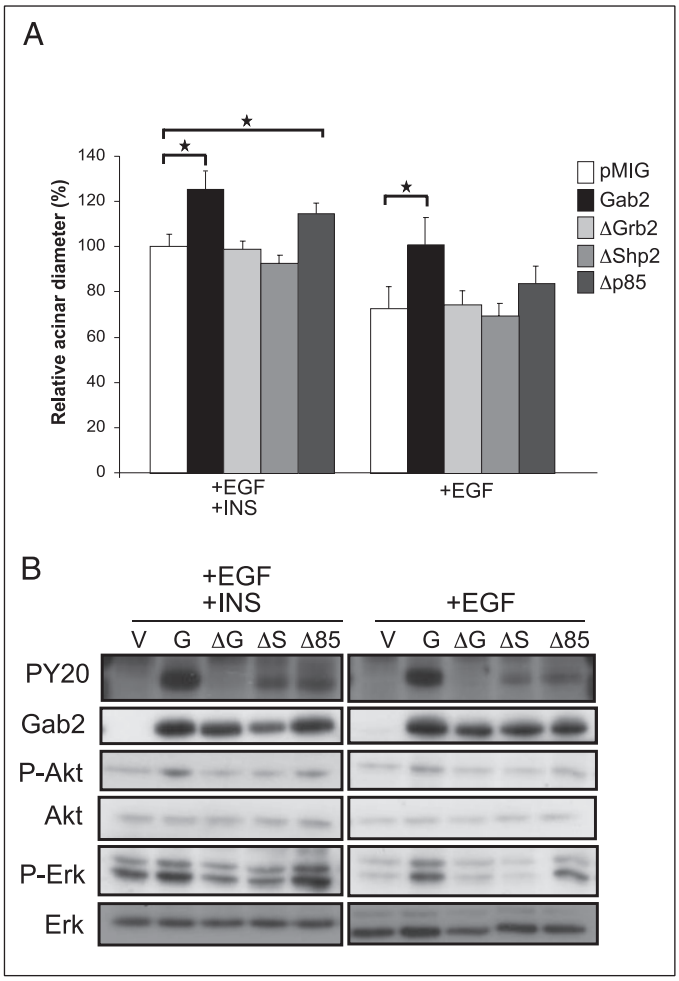

FIGURE 5. **Signaling requirements for Gab2-mediated enhancement of acinar growth.** *A*, effect of Gab2 mutants on acinar diameter. MCF-10A cells expressing either wild-type Gab2 or different Gab2 mutants were cultured in Matrigel under the indicated conditions for 6 days. The mean acinar diameter from three independent experiments, with 80 structures/cell line/time point analyzed in each experiment, is expressed as a percentage relative to vector controls. The *error bars* indicate S.E. *, $p < 0.05$. *INS*, insulin. *B*, effect of Gab2 mutants on cell signaling. Lysates from three-dimensional cultures at Day 4 were subjected to Western blotting with the indicated antibodies. The PY20 blot shows a band of ~95 kDa that represents the tyrosine-phosphorylated Gab2 protein, as confirmed by subsequent stripping and reprobing with anti-Gab2 antibody. *V*, vector; *G*, wild-type Gab2; *ΔG*, ΔGrb2; *ΔS*, ΔShp2; *Δ85*, Δp85; *P*, phospho.

ited a modest, but statistically significant increase in Akt activation upon Gab2 overexpression (23%, $p = 0.01$). A smaller, but non-significant enhancement of Akt phosphorylation was also detected for the Δp85 mutant, whereas no effect was observed for the ΔGrb2 and ΔShp2 mutants. Similar trends were evident for cells grown with EGF only, although the increase in Akt activation upon Gab2 overexpression was smaller and did not reach statistical significance. Because the Δp85 mutant was not as effective as wild-type Gab2 in enhancing acinar size under both growth conditions (Fig. 5*A*), but induced similar levels of Erk activation (Fig. 5*B*), this indicates that activation of PI3K by Gab2/p85 binding contributes to the effect of Gab2 on cell proliferation in three-dimensional culture.

Evaluation of the Contribution of Erk Signaling to Gab2-mediated Enhancement of Acinar Size—To more directly test the role of Erk in acinar growth enhancement by Gab2, we employed the MEK inhibitor U0126. For cells stimulated with a combination of EGF and insulin, careful titration of this compound enabled us to reduce Erk activation in Gab2-overexpressing acini to levels equivalent to those detected in vehicle-treated control acini, without effects on Gab2 expression or Akt activation (Fig. 6*A*, compare Erk activation for Gab2-infected cells at 0.5 μM U0126 with Me_2SO-treated vector cells). This consistently resulted in a modest reduction of acinar size ($p = 0.053$ using the combined data from three independent experiments), indicating that the Erk pathway does contribute to Gab2-mediated growth enhancement. However, in the presence of this concentration of U0126, the Gab2-overexpressing acini were still significantly larger than controls (Fig. 6*B*). Therefore, to extend these analyses, we examined the combined contribution from Gab2/p85 binding and Erk activation. However, a similar degree of MEK inhibition in acini expressing the Δp85 mutant did not affect acinar diameter (Fig. 6, *C* and *D*), which may indicate that Akt activation is growth-limiting for these cells. Also, because acini expressing the Δp85 mutant and treated with U0126 were still larger than controls, Gab2 must promote growth by one or more mechanisms independent of p85 binding and Erk activation.

Gab2 Overexpression Results in Independence of the Acinar Morphogenetic Program from Exogenous EGF—The ability of Gab2 to partially substitute for insulin in the early stages of acinar development (Fig. 3) led us to perform a more stringent test of the effect of Gab2 on growth factor sensitivity and to determine its ability to compensate for the absence of EGF. The previous work of Brugge and co-workers (34) has determined that only expression of certain oncogene combinations (*e.g.* activated Akt and cyclin D_1) will drive formation of acinar structures under these conditions. Consistent with these data, vector control cells grown in the presence of only insulin formed small clusters of cells that lacked structural organization. However, ~50% of the MCF-10A/Gab2 cells formed much larger structures that developed hollow lumina due to apoptosis of centrally located cells (Fig. 7, *A–C*). At Day 4, weak tyrosine phosphorylation of Gab2 could be detected in these acini, along with enhanced Erk activation and an increased proportion of cells in S phase relative to controls (Fig. 7*D* and data not shown). Determination of the signaling requirements for Gab2-stimulated acinar growth under these conditions revealed a contribution from p85 binding and a dependence on recruitment of Grb2 and Shp2 (Fig. 7*E*). Acinar morphogenesis was not observed upon expression of any of the mutants (data not shown). Unfortunately, we could not obtain reproducible data for activation of downstream pathways by these mutants because only very small amounts of protein could be isolated from the cultures.

To eliminate the possibility that Gab2-stimulated acinar growth under these conditions was in response to a low concentration of residual EGF present in the culture medium or to autocrine EGFR ligands, we tested the effect of gefitinib, a selective EGFR tyrosine kinase inhibitor. Addition of 0.5 μM gefitinib to three-dimensional cultures markedly reduced EGF-induced EGFR and Gab2 tyrosine phosphorylation, without affecting Gab2 protein levels (data not shown). However, for cells maintained in medium containing insulin alone, this concentration of gefitinib did not prevent Gab2-mediated growth enhancement (Fig. 7*F*), and the spheroids still underwent normal morphogenesis (data not shown). These data confirm that the effects of Gab2 in insulin-only cultures are independent of EGFR kinase activity.

Further Elevation of Gab2 Expression Results in a More Advanced Phenotype—As described above, we originally generated three pools of MCF-10A cells designated as low, moderate, and high expressors of Gab2 (Fig. 1*A*). To evaluate the oncogenic potential of Gab2 in more detail, we characterized the "high expressing" pool. This level of Gab2 expression led to a more marked amplification of intracellular signaling, as indicated by the enhanced Erk activation in unstimulated cells as well as in cells treated with EGF for 1 and 5 min (Fig. 8*A*). This is in contrast

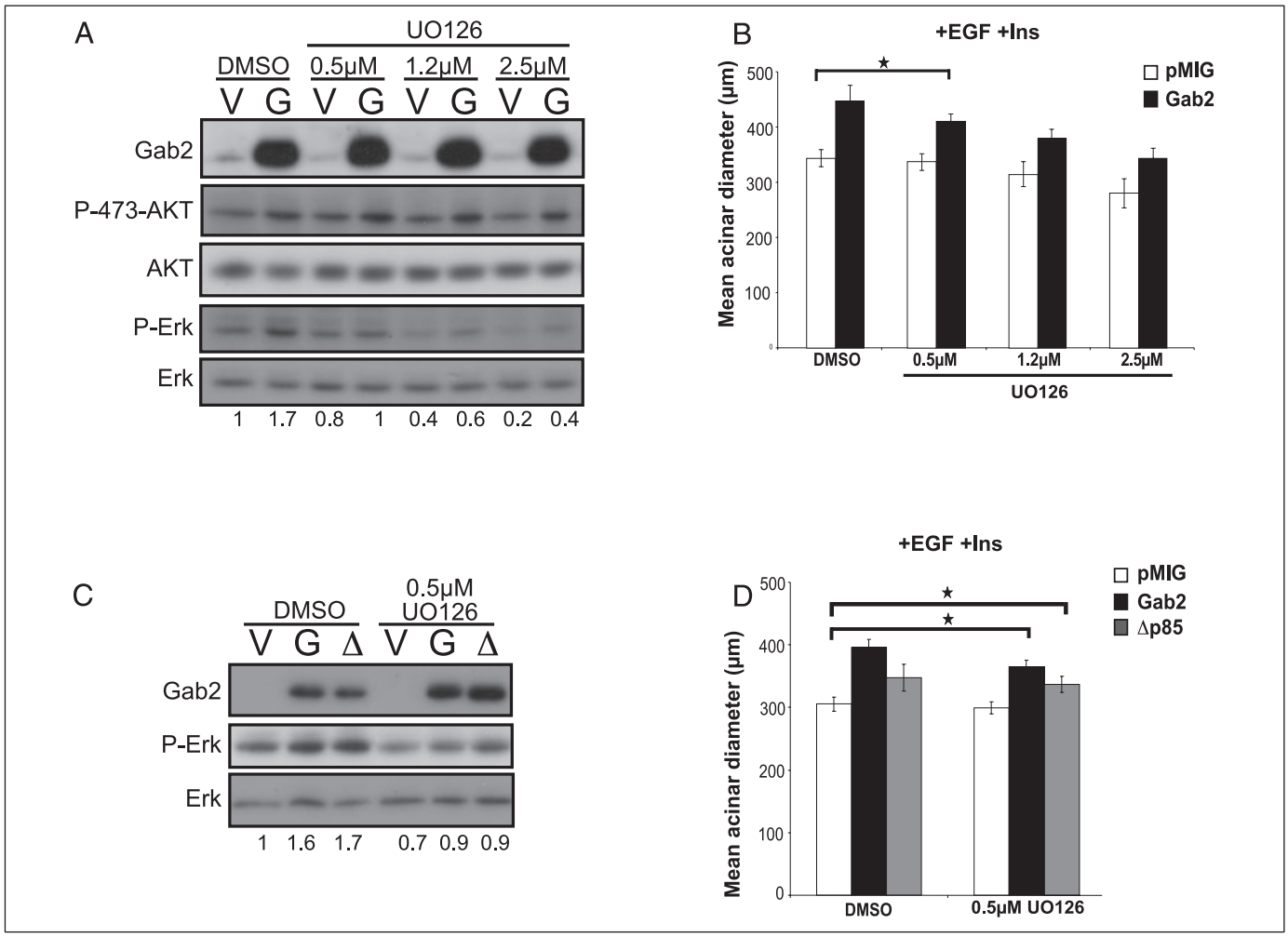

FIGURE 6. **Effect of pharmacological inhibition of MEK on acinar growth.** *A*, effect of U0126 on protein expression and signaling. Vector control (*V*) or Gab2-overexpressing (*G*) MCF-10A cells were maintained in three-dimensional culture in the presence of EGF and insulin and either Me_2SO (*DMSO*; vehicle control) or the indicated concentration of the MEK inhibitor U0126. Cell lysates derived from acini at Day 4 were then Western-blotted with the indicated antibodies. The *numbers* below each lane indicate relative Erk activation normalized for total protein levels, with the level for vehicle-treated vector cells arbitrarily set at 1.0. *P-473-Akt*, phospho-Ser^{473} Akt; *P-Erk*, phospho-Erk. *B*, effect of U0126 on Gab2-enhanced acinar growth. The mean acinar diameter at Day 5 for cells grown as described for *A* is shown. The data are representative of three independent experiments, each performed as in the legend to Fig. 5*A*. The *error bars* indicate S.E. *, $p < 0.05$. *Ins*, insulin. *C*, effect of U0126 on signaling in MCF-10A cells expressing wild-type Gab2 or the Δp85 mutant (Δ). *D*, effect of MEK inhibition on acinar growth of the cells utilized in *C*. Acinar growth was analyzed as described for *B*.

to the "low expressing" pool, in which effects of Gab2 on Erk were observed only at 15 min and later (Fig. 1*B*). Upon monolayer culture, the high expressing cells exhibited an enhancement of the EGF-induced proliferation rate similar to the low expressing cells (data not shown). However, when grown in Matrigel, ~30% of the high expressing cells formed large disorganized structures with defective luminal clearance and a lack of proliferative suppression. These effects were related to the degree of Gab2 overexpression, as indicated by GFP intensity (Fig. 8*B*). These findings lend further support to the hypothesis that deregulated Gab2 signaling contributes to mammary tumorigenesis.

DISCUSSION

Previous functional analyses of Gab2 have identified roles for this docking protein in mast cell development (35), macrophage and osteoclast differentiation (5, 36) and Fcϵ receptor I-mediated mast cell responses (14). However, the overexpression of Gab2 in a subset of breast cancer cell lines and primary breast cancers (19) raises the important question of its effects on mammary epithelial cells. Therefore, we have addressed this issue using three-dimensional culture of MCF-10A cells, which provides the opportunity to investigate a variety of biological endpoints. Furthermore, we have utilized this model system to characterize a series of Gab2 mutants and thus provide novel insights into the role of particular protein-protein interactions and effector pathways in Gab2 signaling.

Overexpression of Gab2 at a magnitude similar to that observed in breast cancer cells confers three effects on MCF-10A cells in Matrigel culture. First, Gab2 enhances acinar diameter by increasing cell proliferation during the early stages of morphogenesis (Figs. 3 and 7). For cells growing in both EGF and insulin, Gab2/p85 binding (leading to stimulation of PI3K) and enhanced Erk activation both contribute to this effect (Figs. 5 and 6). These findings are consistent with the increased proliferation in MCF-10A acini expressing activated Akt (34) and the requirement for Erk in alveolar morphogenesis (37). Second, Gab2 overcomes the proliferative suppression that normally occurs in late stage cultures (Fig. 3). Interestingly, this does not occur upon expression of activated Akt alone (34), indicating that other pathways downstream of Gab2 must contribute to this effect. Finally, Gab2 overexpression results in independence of the morphogenetic program from exogenous EGF, so, in the presence of insulin only, the resulting structures are smaller than those observed upon culture with EGF, but still display a normal

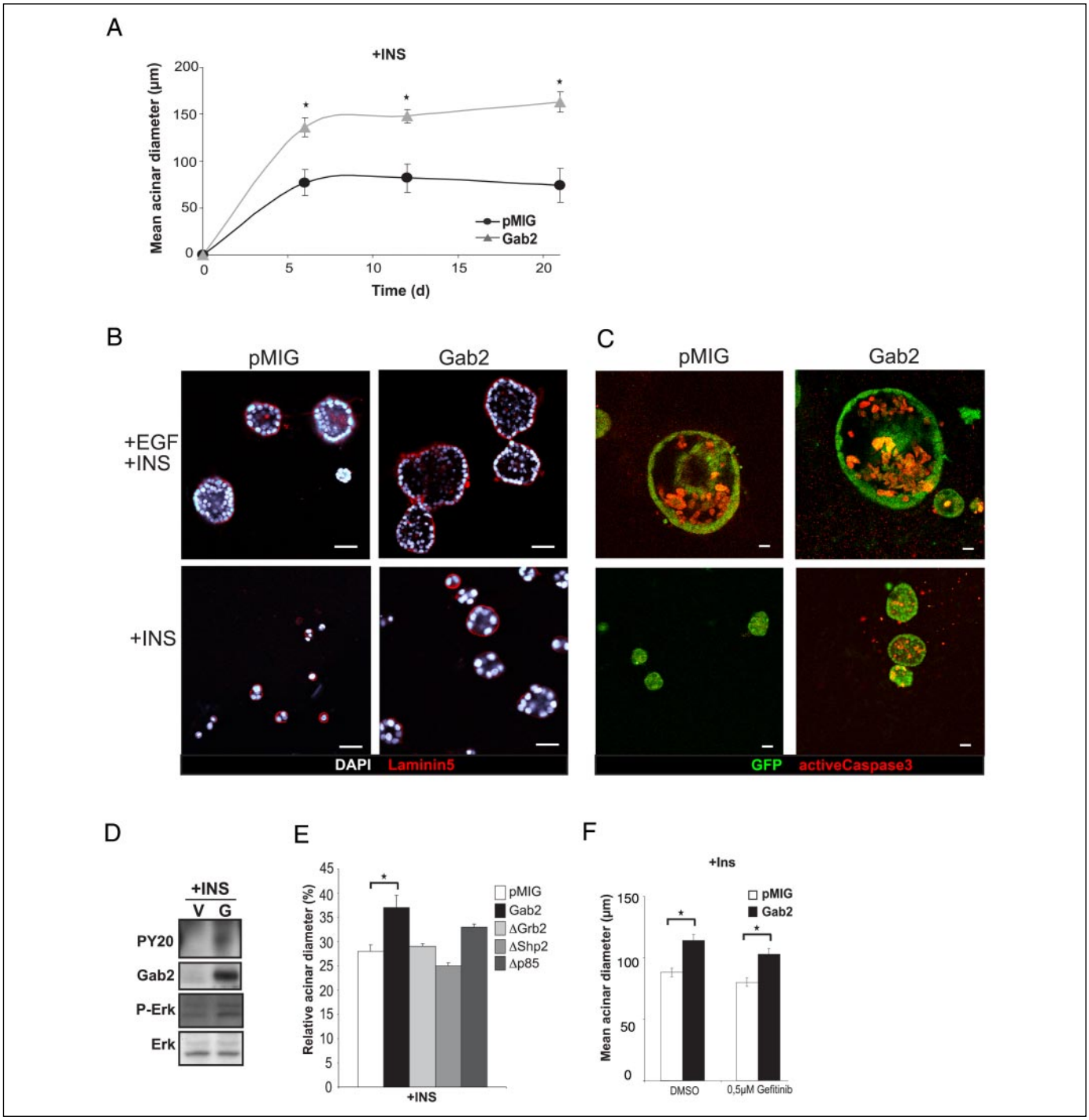

FIGURE 7. **Gab2 overexpression results in EGF-independent acinar morphogenesis.** *A*, effect of Gab2 on EGF-independent acinar growth. Control or Gab2-overexpressing MCF-10A cells were maintained in three-dimensional Matrigel cultures in culture medium containing only insulin (+*INS*), and the mean acinar diameter was assessed over 21 days. Each point represents the mean acinar diameter from three independent experiments. In each experiment, 150 acini were analyzed per time point. *B* and *C*, effect of Gab2 on EGF-independent acinar morphogenesis. Gab2-overexpressing and vector control cells were cultured in three-dimensional culture medium supplemented with insulin (*lower panels*) or with EGF and insulin (*upper panels*). Representative equatorial confocal cross-sections through laminin-5 (*red*)- and 4′,6-diamidino-2-phenylindole (*DAPI*; *white*)-stained structures at Day 21 are shown in *B*. *Scale bars* = 40 μm. Equivalent sections for acini at Day 14 stained for active caspase-3 (*red*) are shown in *C*. *Scale bars* = 40 μm. *D*, effect of Gab2 on signaling in three-dimensional cultures supplemented with insulin. Day 4 lysates were subjected to Western blotting with the indicated antibodies. *V*, vector; *G*, Gab2; *P-Erk*, phospho-Erk. *E*, signaling requirements for Gab2-induced, EGF-independent acinar growth. MCF-10A cells expressing either wild-type Gab2 or different Gab2 mutants were cultured in three-dimensional culture medium supplemented with only insulin for 6 days. Acinar growth was analyzed as described in the legend to Fig. 5*A* and is expressed as a percentage relative to vector control cells maintained with EGF and insulin. *F*, effect of gefitinib on EGF-independent growth. Cells were cultured for 6 days as described for *A* in the presence of gefitinib or Me_2SO (*DMSO*; vehicle control). Acinar diameter was then determined as described for *A*. For *A*, *E*, and *F*, the *error* bars represent S.E. *, $p < 0.05$.

architecture and hollow lumen (Fig. 7). Certain aspects of the phenotype resulting from Gab2 overexpression resemble the effects of introducing the human papilloma virus-16 E7 oncoprotein into MCF-10A cells; this also results in larger acini with a normal lumen that escape proliferative suppression (23). However, E7 expression is insufficient to promote EGF-independent proliferation and morphogenesis (34).

The ability of Gab2 to modulate growth factor sensitivity has also been observed in myeloid cells, in which Gab2 is required for either the

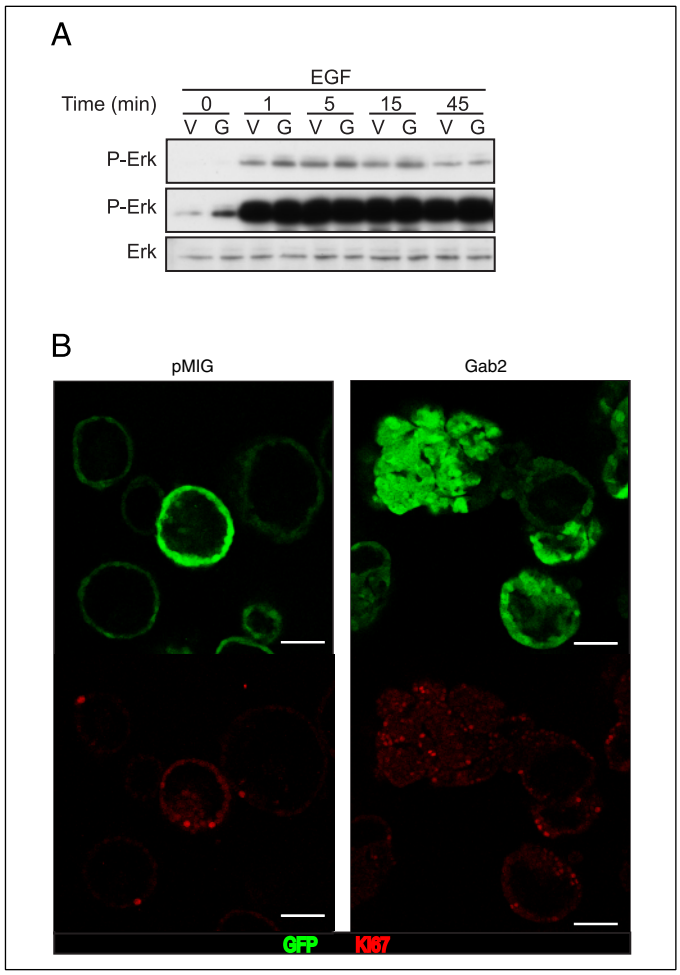

FIGURE 8. **Signaling and acinar morphogenesis in the high expressing pool of retrovirally infected MCF-10A cells.** *A*, EGF-induced Erk activation. Cells were serum-starved and then treated with EGF for the indicated times. Cell lysates were blotted with the indicated antibodies. The *middle panel* shows a longer exposure of the blot presented in the *upper panel*. *V*, vector; *G*, Gab2; *P-Erk*, phospho-Erk. *B*, acinar morphogenesis in the presence of EGF and insulin. GFP fluorescence (*upper panels*) and Ki67 staining (*lower panels*) for control and Gab2-overexpressing cells at Day 23 are shown. *Scale bars* = 80 μM.

Shp2 E76K or Bcr-Abl oncoprotein to induce factor independence (17, 18), and is likely to reflect the ability of Gab2 to amplify multiple signaling pathways. Because the Δp85 mutant of Gab2 cannot promote acinar morphogenesis in insulin-only cultures, one of these must be PI3K/Akt. This is consistent with the observation that coexpression of activated Akt with E7 overrides the dependence of the MCF-10A morphogenetic program on EGF (34). However, activated Akt alone cannot promote EGF independence (34), indicating that other pathways must contribute. This is supported by the requirement for Shp2 binding by Gab2 (Fig. 7*E*). Potential candidates are Stat5 (discussed below) and NF-κB, which has recently been demonstrated to function downstream of Gab2 (5). Also, it should be noted that high expression of Gab2 may promote c-Src activation via either Shp2 activation (10) or direct association (38) and that, in the Matrigel culture system, Gab2 may amplify integrin-derived signals (4). Therefore, the observed effect of Gab2 on MCF-10A cells growing in the presence of only insulin is likely to reflect its role in these pathways as well as its coupling to the activated insulin receptor and insulin-like growth factor-1 receptor.

Despite the proliferative effects of Gab2, this docking protein (like E7) does not prevent luminal clearance (Fig. 3). The oncogenes *erbB2* and v-*src* induce luminal filling via Erk-mediated down-regulation of the pro-apoptotic protein Bim (39). Although Gab2-overexpressing acini exhibit increased levels of activated Erk (Fig. 5), this must be insufficient to down-regulate Bim and to prevent apoptosis of luminal cells. Indeed, because late stage Gab2-overexpressing acini display an increased proportion of apoptotic cells, as determined by anti-active caspase-3 staining (data not shown), Gab2 may promote the activation of alternative pro-apoptotic signaling pathways. One possibility (supported by the increased levels of phospho-Rb in Gab2-overexpressing cells) (Fig. 3) is the activation of E2F transcription factors, leading to expression of pro-apoptotic genes (40). Presumably, the robust Erk activation observed in the high expressing Gab2 pool (Fig. 8*A*) is sufficient to inhibit Bim expression and hence luminal clearance (Fig. 8*B*).

The MCF-10A system also provided a novel and powerful model system to characterize the biological activity of a series of Gab2 binding site mutants. Because receptor co-immunoprecipitation was markedly reduced for the ΔGrb2 mutant (Fig. 4*B*), Grb2 is required for Gab2 recruitment to the EGFR, as it is for Gab2 binding to c-Met (41). However, because introduction of the ΔGrb2 mutation also resulted in loss of EGF-induced Shc binding (Fig. 4*C*) and because the EGFR binds directly to both Shc and Grb2 (42), Gab2 may be coupled to the EGFR by either Grb2 alone or a Grb2·Shc complex. Both modes have been reported for recruitment of Gab proteins to particular receptors (3). Interestingly, the ΔGrb2 mutant is initially tyrosine-phosphorylated in response to EGF (Fig. 4*A*), but this effect is transient, presumably indicating that stable association with the EGFR is required to maintain tyrosine phosphorylation in the presence of protein-tyrosine phosphatase activity. Indeed, in three-dimensional cultures, tyrosine phosphorylation of the ΔGrb2 mutant was undetectable (Fig. 5*B*). Consistent with this finding, the ΔGrb2 mutant was unable to promote acinar growth under any of the growth conditions examined (Figs. 5 and 7). Interestingly, Grb2 binding to Gab2 was also required for acinar growth and morphogenesis in the presence of insulin (Fig. 7*E*). Because Grb2 is not thought to bind the insulin receptor and insulin-like growth factor-1 receptor directly, one possibility to explain this observation is the assembly of an insulin receptor substrate-1·Grb2·Gab2 complex. A precedent for this is the formation of a fibroblast growth factor receptor substrate-2·Grb2·Gab1 complex in fibroblast growth factor receptor signaling (43).

The two other Gab2 binding partners that we investigated were the protein-tyrosine phosphatase Shp2 and the p85 subunit of PI3K. Recruitment of Shp2 by Gab proteins is critical for Erk activation in response to a variety of stimuli (3), and expression of Shp2 binding-defective Gab2 proteins in hepatocytes (38) and breast cancer cells (44) inhibits EGF-induced activation of this pathway. As expected from the role of Shp2 as a positive regulator of Ras, the ΔShp2 mutant of Gab2 was unable to promote Erk activation in three-dimensional culture (Fig. 5*B*). Interestingly, Grb2 binding was reduced for the ΔShp2 mutant (Fig. 4*C*), an observation consistent with a previous report describing a requirement for Shp2 for optimal Grb2 binding by Gab1 (45). This may indicate that a kinase that phosphorylates Grb2 SH2 domain-binding sites on Gab2 is positively regulated by Shp2 or that Grb2 binds via its SH2 domain to Gab2-bound, tyrosine-phosphorylated Shp2 (46). Either mode would provide an additional mechanism whereby Gab2 regulates Ras/Erk signaling.

However, Gab2/Shp2 binding is also important for cytokine-induced immediate-early gene activation independent of its effect on Erk (47), indicating at least one additional signaling function. Of interest in this regard, introduction of the ΔShp2 mutation also reduced the ability of Gab2 to enhance Akt activation (Fig. 5*B*). Work by Neel and co-workers (45) has revealed a complex interplay between Shp2 and activation of PI3K in fibroblasts, with Shp2 negatively regulating PI3K signaling in response to EGF, but playing a positive role upon cellular stimulation with platelet-derived growth factor or insulin-like growth factor-1. For

MCF-10A epithelial cells under our culture conditions, positive effects of Shp2 on PI3K activation must predominate. Possible mechanisms include Shp2-mediated activation of a kinase that phosphorylates the p85-binding sites on Gab2 and an indirect effect via Ras, which, in its GTP-bound form, binds and activates the PI3K p110 catalytic subunit (48). Operation of both mechanisms would explain why the ΔShp2 mutations appear to have a more deleterious effect on Akt activation than loss of the p85-binding sites (Fig. 5*B*). The inability of the ΔShp2 mutant of Gab2 to enhance activation of either Erk or Akt is consistent with its lack of effect on proliferation (Figs. 5 and 7).

For cells maintained in the presence of both EGF and insulin, deletion of the p85-binding sites on Gab2 impaired the ability of this docking protein to promote Akt activation and to increase acinar size (Figs. 5*A* and 6*D*). Because loss of p85 binding did not affect Erk activation (Fig. 5*B*), these data indicate that activation of PI3K via Gab2/p85 binding contributes to promotion of acinar growth. However, the size of acini expressing the Δp85 mutant of Gab2 was not altered when Erk activity was reduced to control values by MEK inhibition (Fig. 6, *C* and *D*). The residual effect of the Δp85 mutant on acinar size could be due to enhancement of PI3K activation by a mechanism independent of Gab2/p85 binding, *e.g.* via Ras, because a small increase in Akt activation was detectable in cells expressing the Δp85 mutant (Fig. 5*B*). Alternatively, Gab2 may promote activation of one or more downstream pathways in addition to Erk and Akt. One possibility is the Stat5 pathway, which positively regulates cyclin D_1 expression and thus may stimulate cell cycle progression (49). A potential link between Shp2 and Stat5 is provided by c-Src, which is activated by Shp2 (10) and can tyrosine-phosphorylate Stat5b, leading to its nuclear translocation (49). Also, Shp2 complexes with Stat5 and migrates with it into the nucleus (49). In support of this hypothesis, elevated Stat5 tyrosine phosphorylation is observed in cells expressing the leukemogenic Shp2 mutant E76K (18), and we observed increased basal Stat5 phosphorylation in Gab2-overexpressing MCF-10A cells (Fig. 1*B*). To summarize, enhanced activation of Erk (due to Shp2 binding) and PI3K/Akt (due to both Shp2 and p85 binding) contributes to enhancement of acinar growth by Gab2, but we cannot rule out a contribution from at least one other pathway.

The ability of Gab2 to stimulate cell cycle progression, to override proliferative suppression, and to induce growth factor independence is consistent with a role for this protein in mammary tumorigenesis. Because activating Shp2 mutations have been detected in certain leukemias and solid tumor types (50), Gab2 overexpression may represent an alternative mechanism to amplify this signaling pathway. Although inhibition of luminal clearance in MCF-10A acini occurred only upon further elevation of Gab2 expression, this may indicate that the levels of tyrosine-phosphorylated Gab2 must be increased above a particular threshold for oncogenic transformation to occur. This is consistent with the biological activity of the Gab2 S159A mutant, which is transforming in fibroblasts and exhibits enhanced tyrosine phosphorylation due to loss of negative feedback regulation (15). Notably, several receptor and non-receptor tyrosine kinases that couple to Gab2 exhibit enhanced expression and/or activity in breast cancer, including ErbB2 and c-Src (21, 51). Therefore, the cooperation between such kinases and Gab2 in malignant transformation of breast epithelial cells will be an important area for future study.

Acknowledgments—We thank Dr. Clare Gordon-Thomson (University of Western Sydney) for assistance with provision of reagents, Drs. Warren Pear (University of Pennsylvania, Philadelphia, PA) and Sebastian Herzog (Max Planck Institute for Immunobiology, Freiburg, Germany) for providing the pMIG vector and related sequence information, and Sheena Gordon for technical assistance.

REFERENCES

1. Schlessinger, J. (2000) *Cell* **103,** 211–225
2. Liu, Y., and Rohrschneider, L. R. (2002) *FEBS Lett.* **515,** 1–7
3. Gu, H., and Neel, B. G. (2003) *Trends Cell Biol.* **13,** 122–130
4. Yu, W. M., Hawley, T. S., Hawley, R. G., and Qu, C. K. (2002) *Blood* **99,** 2351–2359
5. Wada, T., Nakashima, T., Oliveira-dos-Santos, A. J., Gasser, J., Hara, H., Schett, G., and Penninger, J. M. (2005) *Nat. Med.* **11,** 394–399
6. Lock, L. S., Frigault, M. M., Saucier, C., and Park, M. (2003) *J. Biol. Chem.* **278,** 30083–30090
7. Agazie, Y. M., and Hayman, M. J. (2003) *Mol. Cell. Biol.* **23,** 7875–7886
8. Montagner, A., Yart, A., Dance, M., Perret, B., Salles, J. P., and Raynal, P. (2005) *J. Biol. Chem.* **280,** 5350–5360
9. Ren, Y., Meng, S., Mei, L., Zhao, Z. J., Jove, R., and Wu, J. (2004) *J. Biol. Chem.* **279,** 8497–8505
10. Zhang, S. Q., Yang, W., Kontaridis, M. I., Bivona, T. G., Wen, G., Araki, T., Luo, J., Thompson, J. A., Schraven, B. L., Philips, M. R., and Neel, B. G. (2004) *Mol. Cell* **13,** 341–355
11. Seiffert, M., Custodio, J. M., Wolf, I., Harkey, M., Liu, Y., Blattman, J. N., Greenberg, P. D., and Rohrschneider, L. R. (2003) *Mol. Cell. Biol.* **23,** 2415–2424
12. Itoh, M., Yoshida, Y., Nishida, K., Narimatsu, M., Hibi, M., and Hirano, T. (2000) *Mol. Cell. Biol.* **20,** 3695–3704
13. Sachs, M., Brohmann, H., Zechner, D., Muller, T., Hulsken, J., Walther, I., Schaeper, U., Birchmeier, C., and Birchmeier, W. (2000) *J. Cell Biol.* **150,** 1375–1384
14. Gu, H., Saito, K., Klaman, L. D., Shen, J., Fleming, T., Wang, Y., Pratt, J. C., Lin, G., Lim, B., Kinet, J.-P., and Neel, B. G. (2001) *Nature* **412,** 186–190
15. Lynch, D. K., and Daly, R. J. (2002) *EMBO J.* **21,** 72–82
16. Ischenko, I., Petrenko, O., Gu, H., and Hayman, M. J. (2003) *Oncogene* **22,** 6311–6318
17. Sattler, M., Mohi, M. G., Pride, Y. B., Quinnan, L. R., Malouf, N. A., Podar, K., Gesbert, F., Iwasaki, H., Li, S., Van Etten, R. A., Gu, H., Griffen, J. D., and Neel, B. G. (2002) *Cancer Cell* **1,** 479–492R. A. V.
18. Mohi, M. G., Williams, I. R., Dearolf, C. R., Chan, G., Kutok, J. L., Cohen, S., Morgan, K., Boulton, C., Shigematsu, H., Keilhack, H., Akashi, K., Gilliland, D. G., and Neel, B. G. (2005) *Cancer Cell* **7,** 179–191
19. Daly, R. J., Gu, H., Parmar, J., Malaney, S., Lyons, R. J., Kairouz, R., Head, D. R., Henshall, S. M., Neel, B. G., and Sutherland, R. L. (2002) *Oncogene* **21,** 5175–5181
20. Troyer, K. L., and Lee, D. C. (2001) *J. Mammary Gland Biol. Neoplasia* **6,** 7–21
21. Salomon, D. S., Brandt, R., Ciardiello, F., and Normanno, N. (1995) *Crit. Rev. Oncol. Hematol.* **19,** 183–232
22. Shaw, K. R., Wrobel, C. N., and Brugge, J. S. (2004) *J. Mammary Gland Biol. Neoplasia* **9,** 297–310
23. Debnath, J., Mills, K. R., Collins, N. L., Reginato, M. J., Muthuswamy, S. K., and Brugge, J. S. (2002) *Cell* **111,** 29–40
24. Muthuswamy, S. K., Li, D., Lelievre, S., Bissell, M. J., and Brugge, J. S. (2001) *Nat. Cell Biol.* **3,** 785–792
25. Wrobel, C. N., Debnath, J., Lin, E., Beausoleil, S., Roussel, M. F., and Brugge, J. S. (2004) *J. Cell Biol.* **165,** 263–273
26. Wu, Y., Hayes, V. M., Osinga, J., Mulder, I. M., Looman, M. W., Buys, C. H., and Hofstra, R. M. (1998) *Nucleic Acids Res.* **26,** 5432–5440
27. Hayes, V. M., Wu, Y., Osinga, J., Mulder, I. M., van der Vlies, P., Elfferich, P., Buys, C. H., and Hofstra, R. M. (1999) *Nucleic Acids Res.* **27,** e29
28. Van Parijs, L., Refaeli, Y., Lord, J. D., Nelson, B. H., Abbas, A. K., and Baltimore, D. (1999) *Immunity* **11,** 281–288
29. Lock, L. S., Royal, I., Naujokas, M. A., and Park, M. (2000) *J. Biol. Chem.* **275,** 31536–31545
30. Debnath, J., Muthuswamy, S. K., and Brugge, J. S. (2003) *Methods* **30,** 256–268
31. Brummer, T., Elis, W., Reth, M., and Huber, M. (2004) *Methods Mol. Biol.* **271,** 189–212
32. Janes, P. W., Daly, R. J., deFazio, A., and Sutherland, R. L. (1994) *Oncogene* **9,** 3601–3608
33. Soule, H. D., Maloney, T. M., Wolman, S. R., Peterson, W. D., Jr., Brenz, R., McGrath, C. M., Russo, J., Pauley, R. J., Jones, R. F., and Brooks, S. C. (1990) *Cancer Res.* **50,** 6075–6086
34. Debnath, J., Walker, S. J., and Brugge, J. S. (2003) *J. Cell Biol.* **163,** 315–326
35. Nishida, K., Wang, L., Morii, E., Park, S. J., Narimatsu, M., Itoh, S., Yamasaki, S., Fujishima, M., Ishihara, K., Hibi, M., Kitamura, Y., and Hirano, T. (2002) *Blood* **99,** 1866–1869
36. Liu, Y., Jenkins, B., Shin, J. L., and Rohrschneider, L. R. (2001) *Mol. Cell. Biol.* **21,** 3047–3056
37. Niemann, C., Brinkmann, V., Spitzer, E., Hartmann, G., Sachs, M., Naundorf, H., and Birchmeier, W. (1998) *J. Cell Biol.* **143,** 533–545
38. Kong, M., Mounier, C., Dumas, V., and Posner, B. I. (2003) *J. Biol. Chem.* **278,** 5837–5844
39. Reginato, M. J., Mills, K. R., Becker, E. B., Lynch, D. K., Bonni, A., Muthuswamy, S. K., and Brugge, J. S. (2005) *Mol. Cell. Biol.* **25,** 4591–4601
40. Muller, H., and Helin, K. (2000) *Biochim. Biophys. Acta* **1470,** M1–M12

41. Lock, L. S., Maroun, C. R., Naujokas, M. A., and Park, M. (2002) *Mol. Biol. Cell* **13,** 2132–2146
42. Batzer, A. G., Rotin, D., Urena, J. M., Skolnik, E. Y., and Schlessinger, J. (1994) *Mol. Cell. Biol.* **14,** 5192–5201
43. Ong, S. H., Hadari, Y. R., Gotoh, N., Guy, G. R., Schlessinger, J., and Lax, I. (2001) *Proc. Natl. Acad. Sci. U. S. A.* **98,** 6074–6079
44. Meng, S., Chen, Z., Munoz-Antonia, T., and Wu, J. (2005) *Biochem. J.* **391,** 143–151
45. Zhang, S. Q., Tsiaras, W. G., Araki, T., Wen, G., Minichiello, L., Klein, R., and Neel, B. G. (2002) *Mol. Cell. Biol.* **22,** 4062–4072
46. Li, W., Nishimura, R., Kashishian, A., Batzer, A. G., Kim, W. J. H., Cooper, J. A., and Schlessinger, J. (1994) *Mol. Cell. Biol.* **14,** 509–517
47. Gu, H., Pratt, J. C., Burakoff, S. J., and Neel, B. G. (1998) *Mol. Cell* **2,** 729–740
48. Rodriguez-Viciana, P., Warne, P. H., Dhand, R., Vanhaesebroeck, B., Gout, I., Fry, M. J., Waterfield, M. D., and Downward, J. (1994) *Nature* **370,** 527–532
49. Clevenger, C. V. (2004) *Am. J. Pathol.* **165,** 1449–1460
50. Bentires-Alj, M., Paez, J. G., David, F. S., Keilhack, H., Halmos, B., Naoki, K., Maris, J. M., Richardson, A., Bardelli, A., Sugarbaker, D. J., Richards, W. G., Du, J., Girard, L., Minna, J. D., Loh, M. L., Fisher, D. E., Velculescu, V. E., Vogelstein, B., Meyerson, M., Sellers, W. R., and Neel, B. G. (2004) *Cancer Res.* **64,** 8816–8820
51. Kairouz, R., and Daly, R. (2000) *Breast Cancer Res.* **2,** 197–202